2006

Ultimate strength of self consolidating concrete bulb tee beams and the evaluation of bond mechanics in prestressed concrete applications

Greg Parent
Lehigh University

Parent, Greg

Ultimate Strength of Self Consolidating Concrete Bulb Tee Beams and the Evaluation...

January 2006

Ultimate Strength of Self Consolidating Concrete Bulb Tee Beams and the Evaluation of Bond Mechanics in Prestressed Concrete Applications

by

Greg Parent, Graduate Student Researcher

Clay Naito, Principal Investigator

A Thesis
Presented to the Graduate and Research Committee
of Lehigh University
in Candidacy for the Degree of
Master of Science

in

Civil Engineering

Lehigh University

December, 2005

1. THESIS SIGNATURE SHEET

This thesis is accepted and approved in partial fulfillment of the requirements for the Master of Science.

Friday, December 09, 2005

Thesis Advisor

Chairperson of Department

2. TABLE OF CONTENTS

3. LIST OF FIGURES

4. LIST OF TABLES

5. FOREWORD

This thesis contains two PCI (Precast Concrete Institute) Journal articles. Both of these articles have been submitted to PCI and are currently under review for publication.

Part 1 of this thesis analyses the use of Self Consolidating Concrete (SCC) in prestressed bridge beams and compares their results with the beams made with High Early Strength concrete (HESC).

Part 2 of this thesis is an evaluation of Bond Mechanics on both SCC and HESC. Part 2 also proposes a new testing method which closely mimics the bond stress in a prestressed beam, but is a simple test to perform and analyze.

Parts 1 and 2 have there own sections covering Abstract, Introduction, Material Properties, etc.,. However, due to the similar topic matter, nearly all of the variables are identical in parts 1 and 2. Therefore, there is only one Appendix for parts 1 and 2.

6. PART 1: ULTIMATE STRENGTH OF SELF CONSOLIDATING CONCRETE BULB TEE BEAMS

6.1. ABSTRACT

As a means to improve quality and increase production rates for concrete operations Self Consolidating Concretes (SCC) have been developed. These materials exhibit a low viscosity allowing for the elimination of mechanical vibration. SCC has been used for a number of years in the architectural and building precast industry; however it has not been used significantly for pre-tensioned bridge members due to stringent material quality control standards specified by state departments of transportation. To address these concerns the performance of full-scale SCC girders were studied. Four 35 foot long bulb tee girders were produced. Two were produced using High Early Strength Concrete (HESC) and two with SCC. All the girders were tested to failure twice, once at each end. The performance of the SCC girders was compared to that of the HESC girders and to code requirements. The response of the HESC and SCC beams were comparable. In no test did the slip of the strand initiate failure of the beam. Both the HESC and SCC girders exceeded the flexure and shear capacities expected by the ACI code. In addition, transfer lengths and in-situ creep and shrinkage effects were lower than expected.

6.2. INTRODUCTION

Self consolidating concrete (SCC) has the potential to provide a higher quality and cost effective alternative to standard concrete mixes used in the precast industry. The flowability of SCC allows for placement in members with highly congested reinforcement or architectural form features. Use of conventional concretes under these circumstances would require a significant amount of internal and external mechanical vibration and may risk incomplete consolidation and formation of voids. The rheological property of SCC eliminates the vibration processes which increases production and lowers labor costs.

SCC is defined herein as a high-performance concrete that has high deformability (hydraulic slump > 10-in.) in its fresh state and can be placed and compacted under its own self weight without applying vibration. While being highly fluid, SCC is sufficiently cohesive to prevent segregation or blockage of aggregates during concrete placement. The enhanced cohesiveness can ensure better suspension of solid particles in the fresh concrete and, therefore, good deformability and filling capability during the spread of fresh concrete through various obstacles. Typically SCC mixtures include mineral additives, such as fly ash and ground granulated blast furnace (GGBF) slag as well as chemical admixtures such as high range water-reducing admixtures (HRWR) and viscosity-modifying admixtures (VMA) to adjust its deformability and cohesiveness. SCC was developed in Japan in the late 1980's for use in areas with highly congested reinforcement [PCI 2003].

SCC has been accepted in a number of countries for many different structural uses. It is ideal for structures that contain congested reinforcement such as columns, walls and specialty items like insulated concrete forms which typically pose many problems with a standard mix concrete. A highly fluid, stable concrete mixture permits faster placement for these structures. Currently SCC is used in a variety of precast applications such as; tanks, columns, footers, architectural concrete, beams, double tee's, etc.,. Some precast plants are reporting using SCC in nearly 100 percent of their production and expect further opportunities for SCC with the industry acceptance of an SCC specification.

Although SCC has gained acceptance from many precast plants, use in department of transportation work is limited due to the lack of research on SCC in full-scale bridge members. To address this concern a program was conducted to examine strength gain and creep and shrinkage resistance of a SCC mix and elastic shortening, slip of strand to concrete, and ultimate flexural / shear strengths of the beams. This paper describes the results of four bulb tee girders, two SCC and two HESC, loaded

to failure by comparing the response to each other and to the requirements of the American Concrete Institute codes [ACI 1997 and 2005].

6.3. RESEARCH PROGRAM OVERVIEW

The program was divided into two phases: 1) qualification of the materials and 2) qualification of full-scale beam performance. The two phases are discussed in detail in the following sections. A control was included in the study design to provide a baseline comparison of behavior for the SCC. The control consisted of a conventional high early strength concrete (HESC) used successfully for over 10 years for production of precast/prestressed members.

6.4. MATERIAL CHARACTERISTICS

One mix design for each type of concrete, HESC and SCC, was developed for the research program. The two mixes are designed to achieve a compressive strength of 6800psi (46.9MPa) within 24 hours from the time of placement and a compressive strength of 8000psi (55.2MPa) at 28-days. The rapid strength gain allows for early release of prestress forces and a short fabrication schedule. The results discussed are with respect to these two mix designs.

6.4.1. Mix Proportions and Constituents

The mixes are designed to meet the Pennsylvania Department of Transportation (PennDOT) HES specification [PennDOT 2004]. For quality assurance, bounds are placed on the mix proportions and quantities. Cement content is limited to 750 to 850 lb/yd^3, water-to-cement ratio is limited to a maximum of 0.4, and the relative volume of coarse aggregate is limited to 34% to 44%. Six 2.75yd^3 (2.1m^3) batches of SCC and six 2.5yd^3(1.9m^3) batches of HESC were made. The mix proportions between batches vary by less than 1.0% and are summarized in Table 1. All properties are within design specifications. To achieve the necessary strength and rheology, the SCC uses the upper bound of cement content and the lower limit of coarse aggregate volume.

ASTM C989 Grade 120 GGBF slag cement is used in combination with Type III cement to reduce costs while improving the mechanical characteristics, workability [Kosmatka et. al. 1988], and durability [Geiseler et. al. 1995] of the material. Slag cement makes up 25% of the cement content in the SCC mix and 35% in the HESC mix. These levels are on order of mix designs used successfully in previous research.

A crushed Diabase stone is used for coarse aggregate. AASHTO [2000] #67 (0.75in. max) and #8 (0.375 in. max) gradations are used for the HESC mix. Due to the presence of elongated stone in the #67 material which can limit flow in densely reinforced areas, only the #8 aggregate is used in the SCC. The use of smaller max aggregate size ensures good workability in the SCC. Natural silica sand is used for the fine aggregate.

A number of admixtures are used to improve the performance and workability of the mix. Both mixes include an ASTM C494 Type F high range water reducer (to improve workability) and an ASTM C260 neutralized vinsol resin admixture (to entrain air). An ASTM C494 Type B retarder is used in the HESC mix to slow set time. To limit segregation in the SCC mix, a commercially available VMA is used.

Table 1: Average concrete proportions		
Material Type	HESC	SCC
Total Cement [lb/yd^3 (kg/m^3)]	750(445)	849(504)
Slag Cement [%]	34	25
Fine Aggregate SSD [lb/yd^3 (kg/m^3)]	1172 (695)	1283(761)
Coarse Aggregate #67 SSD [lb/yd^3 (kg/m^3)]	1383(820)	0
Coarse Aggregate #8 SSD [lb/yd^3 (kg/m^3)]	552(327)	1651(979)
Water / Cement Ratio	0.34	0.32
High Range Water Reducer [oz/yd^3 (ml/m^3)]	60.0(2320)	136.2(5270)
Retarding Admixture [oz/yd^3 (ml/m^3)]	4.0(154)	0
Air Entrainment Admixture (AEA) [oz/yd^3 (ml/m^3)]	2.4(93)	2.0(76)
Viscosity Modifying Admixture [oz/yd^3 (ml/m^3)]	0	16.0(620)
Coarse Aggregate Volume [%]	39	34
Unit Weight [lb/yd^3]	149.8	148.8
Air Content [%]	5.4	5.0
Slump / Spread [in.]	6.3	21.3

6.4.2. Plastic Properties

Both concrete types met the quality control requirements of ASTM and PCI SCC Interim guidelines [PCI 2003]. Air content and unit weights were within design targets for normal weight concrete for use in severe weather environments (Table 1). The SCC mix was evaluated for flowability using the inverted slump cone spread test. The measured spread was lower than the typical targeted range of 22 to 26 inches; however, it was adequate for the bulb tee application. With minor adjustments of admixtures higher spreads can easily be achieved. The concrete capability to flow through dense reinforcement was examined with the J-ring test. Spread through the J-ring decreased from the free spread by a minimal amount (9.3%); no noticeable segregation or piling of aggregate was observed. A visual stability index (VSI) reading was performed to inspect segregation; no evidence of aggregate piling, segregation in slump flow, or mortar halo was observed in the batches (VSI = 0). In two of six batches, minor bleeding was observed resulting in a VSI of 0.5 (well below the 2.0 acceptance level). To further examine the potential for segregation during placement, a columnar segregation test [Daczko 2002] was conducted. The test consists of evaluating how much aggregate settles over a 15 minute period. No segregation was measured (0%).

All full-scale beams and materials samples endured identical placement, curing, and releasing procedures. Within two hours after placement, the concretes were cured with radiant floor heat, maintaining internal temperatures at an average of 140°F (60°C) for 14 hours. During release of prestressing, at 28.5 hours from placement, the internal temperatures decreased to 120°F (48.9°C).

6.4.3. Hardened Properties

The hardened concrete properties were examined systematically throughout the research program. Tests were initiated prior to release of prestress, at an age of 7, 14, and 28-days, and at the ages corresponding to the destructive beam tests. The results of this study are briefly presented here; further information can be found in Naito et. al. [2005].

The compressive qualities were measured both in terms of initial time of set [ASTM C403] and compressive strength [ASTM C39]. SCC reached an initial set in 6.3 hours, while HESC reached an initial set in 5.2 hours. These durations are typical for conventional concrete however for precast production a shorter time is desirable to expedite finishing operations. The longer SCC duration can be accommodated for in plant operations. Furthermore, the initial set follows accepted curing trends [Popovics 1971]. The measured penetration resistance over time is accurately estimated with a power function as shown in Figure 1.

Compressive strength gain for the two concrete mixes were comparable and within expected values. Both concrete mixes gained over 90% of their 28-day compressive strength in the first 24 hours. The strength remained relatively stable for the first 56 days and increased at later ages (Figure 1). This delayed strength gain does not follow conventional expectations and resulted in a poor fit with ACI 209 [1997] predictions. Release and ultimate design strength requirements were met; however, design strength on the HESC mix was achieved only after 80 days. The long-term strength gain can be improved by modification of the heating temperature and/or duration during the first 24 hours

[Freyne 2003]. The HESC mix exhibited a lower strength than the SCC; subsequent data is normalized to provide comparisons.

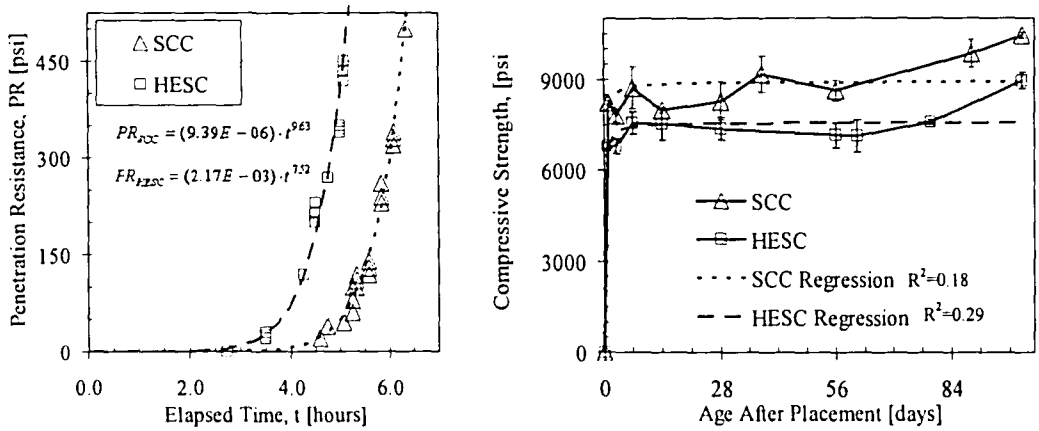

Figure 1: Concrete strength gain

Tension and stiffness properties were evaluated on the match cast cylinders and prisms according to ASTM standards. The splitting tension and modulus of rupture were consistent between the two mixes when normalized to the square root of the compressive strength (Table 2). The modulus of rupture value of 11 was higher than the 7.5 assumed for conventional concretes. The elastic modulus of the SCC was lower than that of the HESC and ACI estimates. This indicates that the formation of tensile cracks associated with flexure and web shear may be delayed while the deformation associated with initial camber and applied loads may be marginally greater than expected.

Table 2: Concrete constitutive properties

Material	Elastic Modulus, E_c		Splitting Tension, f'_t		Modulus of Rupture, f'_r	
	Avg. [ksi]	# of $\sqrt{f'_c}$	Avg. [psi]	# of $\sqrt{f'_c}$	Avg. [psi]	# of $\sqrt{f'_c}$
SCC	5043±131	55402	736	7.7	1066 ± 54	11.1
HESC	5627±136	67590	599	7.1	926 ± 51	11.0

Creep and shrinkage tests were conducted on match cast 6-in x 12-in cylinders. SCC exhibited greater shrinkage and creep than the HESC as illustrated in Figure 2. Both the SCC and HESC exhibit lower shrinkage strain than predicted by the ACI 209 code [ACI 1997]. ACI estimates over-predicted shrinkage by 18% and HESC by 39%. This may be attributed to the low fine aggregate content of both mixes. The SCC exhibited a 39% higher shrinkage strain than the HESC on average. The creep coefficient of the HESC was 6% higher than the ACI prediction. The creep coefficient of the SCC however was approximately 40% higher than ACI predictions. The combined effects of lowered shrinkage and elevated creep in the SCC may cancel each other when examined together in a beam. Despite the variations from code predictions the creep and shrinkage fit well with expected relationships; the resulting formulations are presented as insets in Figure 2.

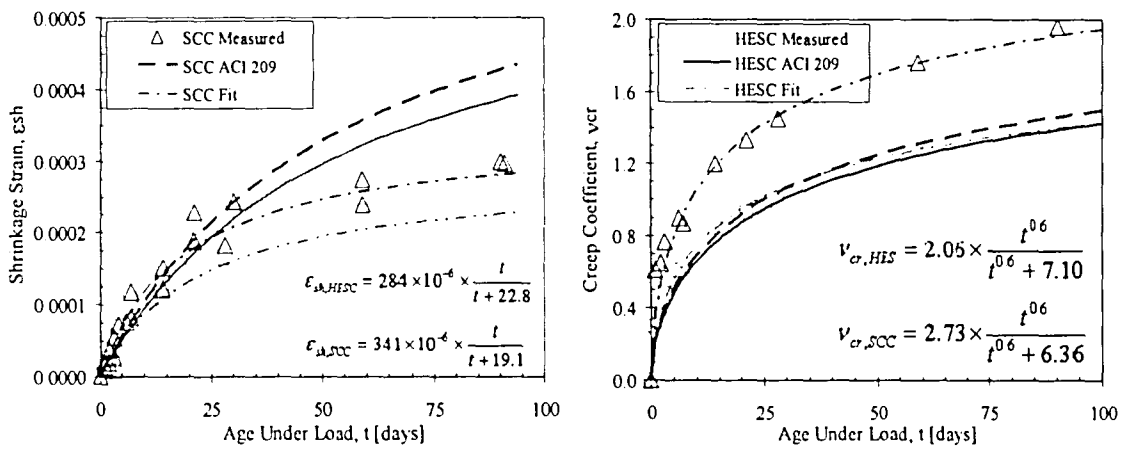

Figure 2: Shrinkage and creep properties

6.5. STRAND AND REINFORCEMENT PROPERTIES

Conventional prestressing strand and reinforcements were used for the research program. Reinforcing steel conformed to the ASTM A615 grade 60 standards. All bars in the concrete were plain, no epoxy coating was used. Two heats of low relaxation 270ksi seven wire ½-in special strands were used in all facets of the project. Reinforcement and strand properties are summarized in Table 3.

Table 3: Reinforcement properties				
Reinforcement Type	Size	Modulus [ksi]	Yield [ksi]	Ultimate [psi]
Continuity	#6	N.A.	72.1	111.0
Stirrups	#4	N.A.	65.8	104.3
Stirrups	#5	N.A.	70.0	101.1
P/S Strand	1/2" Special	28990	260.1	283.3

The strand used for the research study was pre-examined using the large block pullout test requirements summarized in Logan [1997]. A total of 35 pullout tests were conducted on the strand 25 hours after concrete placement. The concrete block achieved the required 4000 psi compressive strength at the time of the pullout tests. The tests were conducted according to specifications at a load rate of approximately 20 kips/min.

Repeatability within a strand group was relatively poor. The coefficient of variation ranged from 9% to 19% for the six rolls of strand examined. The pullout behavior followed a general progression of elastic deformation of the strand with application of load followed by a decrease in stiffness at a load level of approximately 18 kips. This correlates with bond slip of the strand from the concrete. The pullout resistance continued to increase as slip progressed eventually resulting in complete loss of bond capacity. ***All*** strands failed by pullout. On average the ½" special strand achieved a pullout capacity of 31.5 kips with a coefficient of variation of 15%. Previous research [Logan 1997] recommends an acceptable pullout capacity of 36kips for 1/2in. regular strand. Extrapolation to ½" special based on equivalent surface area (computed from the nominal diameter) results in an acceptance level of 37.4 kips for the ½" special strand. All strand pullout values were below the noted acceptance level; however, due to successful past production the strand was included in the testing program.

6.6. BULB TEE SPECIMENS

Bulb tee beam sections with constant tendon eccentricity are examined. The bulb tee geometry was developed through work of the Mid-Atlantic States Prestressed Concrete Committee for Economic

Fabrication (PCEF) and included in the PennDOT standards. The bulb tee measures 45.0-in (114cm) deep and 47.0-in (119cm), wide at the top flange; the as-built dimensions and section properties are presented in Figure 3 and Table 4. A total of 26 strands are used; 24 strands are located in the bulb and 2 in the top flange. All strands are horizontally spaced at a standard distance of 2 inches.

The bulb tee section studied is part of a precast beam production series for a multi-span elevated highway in the Eastern US. Four specimens 35-ft. long are fabricated for the research program: two HESC and two SCC. The section is conventionally topped in the field with an 8.5-in deck slab. The composite slab, however, was not included in the experimental study. The beams are cast in-line and consequently have the same prestressing strand and are subjected to the same curing and release conditions. The de-tensioning operation consisted of a simultaneous release of all the strands over a period of a few minutes.

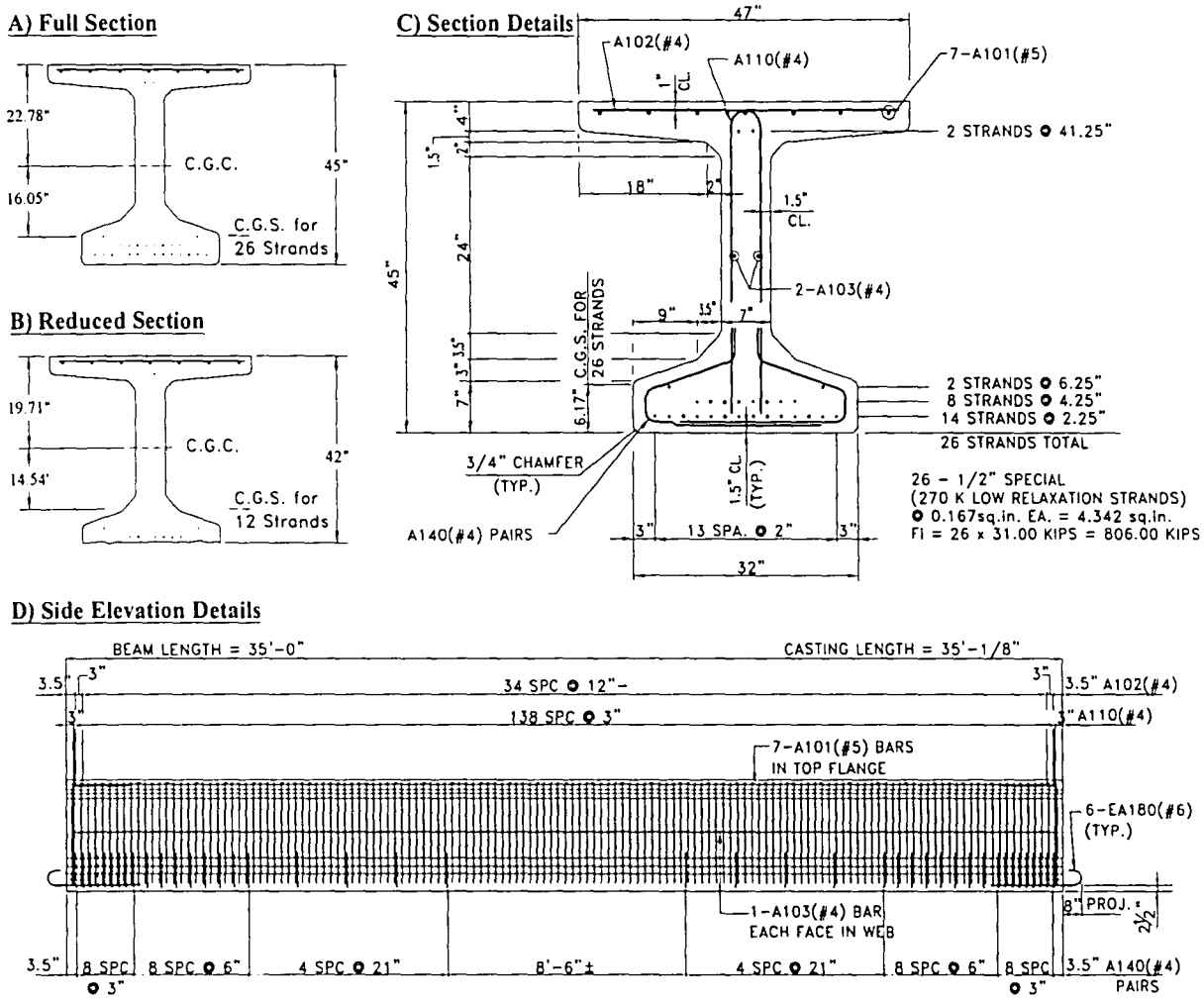

Figure 3: Specimen details

Table 4: Section properties		
Property	Full Section	Reduced Section
Gross Area, A_G	747 in^2	651 in^2
Gross Moment of Inertia, I_G	207,554 in^4	159,300 in^4
Distance to CGS from top, d_P	38.83 in	34.25 in
Distance to CGC from bottom, y_t	22.22 in	25.29 in
Eccentricity of strand, e_p	16.05 in	14.54 in
Total prestressed strand area, A_{ps}	4.342 in^2	2.00 in^2
Uncracked transformed inertia, $I_{g\text{-}tr}$	228,400 in^4	181,600 in^4
Cracked transformed inertia, I_{cr}	28,900 in^4	11,000 in^4

6.7. TEST SETUP

The beams were configured to examine three failure modes: compressive flexural failure (A), shear/flexural failure (B1), and tensile flexural failure (B2). To achieve these failure modes, the beams were tested in two different simply supported configurations, A and B (Figure 4) with two section details, A and B (Figure 3). In all cases, the load was located closer to the roller support. Load was applied using 5000 kip universal testing machine at a quasi-static rate of less than 0.05-in/min. Each beam was first tested in configuration A until failure. The damaged section was then cantilevered off of the loaded span and the beam was retested in configuration B. In configuration A, a flexural span of one development length, L_d, is used. To achieve this, the load is placed at a distance equal to L_d plus the depth of the prestressing strand, d_p (Figure 4A). To achieve a flexural/shear type failure, B1, the distance to the support is reduced as shown in Figure 4 B1. To examine the response under a tensile flexural failure two beams were notched at the load location and the lower 14 strands were severed. With exception to the cutting of the strands at the loading location, all 26 strands were left intact for the rest of the span. The cut section is illustrated in Figure 3B. The strand was severed by locally removing the cover concrete around the lower level of strand and flame cutting them. Adequate concrete protection was left above the cut strands to insulate the upper levels from any accidental heat damage.

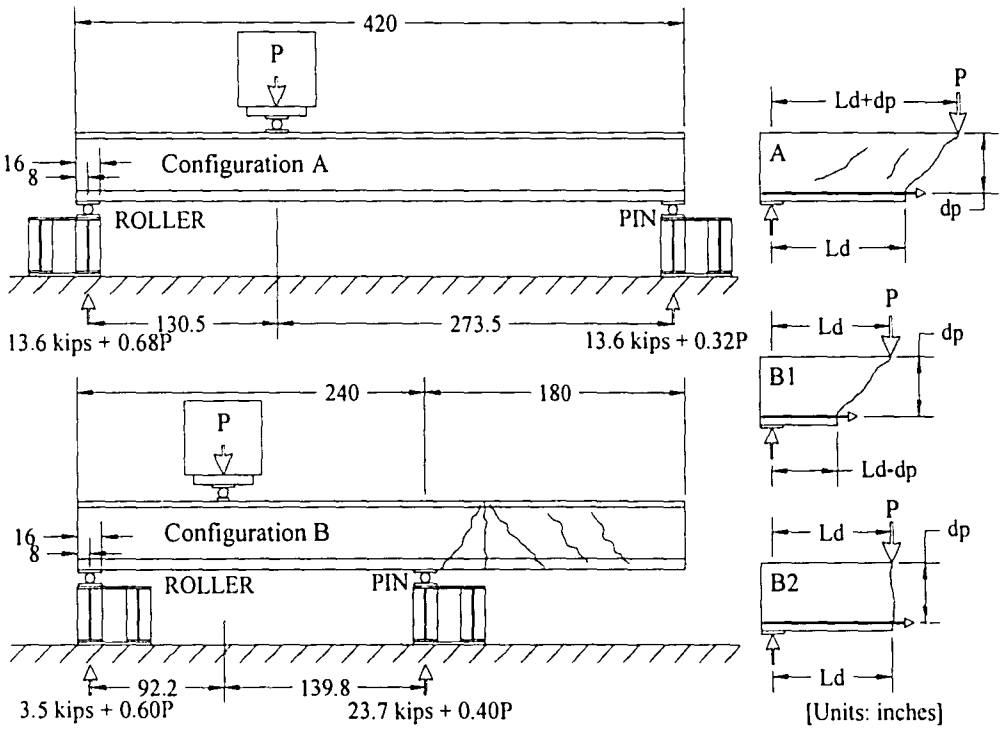

Figure 4: Loading configurations

6.8. EXPERIMENTAL RESULTS

The bulb tee beams were first evaluated in a non-destructive manner to examine the initial camber, creep, shrinkage, elastic response, and transfer length. The specimens were cured for 28-days after which destructive testing began. The destructive tests were conducted from 37 to 111 days after initial concrete placement. Each beam was tested twice resulting in eight destructive tests, six of which are presented in detail (three HESC and three SCC).

6.8.1. Nondestructive Performance

The SCC exhibited a greater stiffness than the conventional HESC mix design and both mixes exceeded ACI estimates (Table 5). The modulus was compared from the measured elastic shortening, camber, and elastic response of the beam. The elastic shortening was measured using embedded vibrating wire strain gages located at the center of the beam span, and a series of resistance based strain gages bonded to the stressed strand prior to de-tensioning. Both elastic shortening and camber

were examined during de-tensioning of the beams. From these measurements and the initial jacking stress of 185.6 ksi, the elastic modulus was computed. Note, the camber was measured with a scale and has limited accuracy. The surface strains measured during elastic loading of the beams are also used with the applied load to compute an elastic modulus. The results of all in-situ tests are contrary to previous cylinder tests. The discrepancy between in-situ and beam tests could be attributed to the post 24-hour cure techniques; the cylinders were kept moist according to ASTM requirements while the beam was left to cure in an exposed condition at the precast plant storage yard.

Table 5: In-situ modulus of concrete [ksi]				
Material	Elastic Shortening	Camber	Surface Strain	ACI Estimate for f'_c = 8 ksi
SCC	5375±185	5900±1600	5660±220	5098
HESC	4880±203	3900±700	5508±12	

The in-situ creep and shrinkage properties were monitored in the beams using vibrating wire strain gages as previously discussed. The data represents the strains measured in both HESC and both SCC beams. The prestressed beams experienced less creep and shrinkage than ACI predictions (Figure 5A). Furthermore, the SCC beam experienced less creep and shrinkage than the HESC beam. From these observations one can conclude that the SCC provides greater resistance than HESC to the combined effects of creep and shrinkage when used in bulb tee beams.

The effective prestress is considerably higher than PCI predictions. The effective prestress is approximated using the embedded vibrating wire strain data. Since the gauge is located in the center of the beam span the assumption is made that no slip occurs between the strand and the concrete. Consequently, the strain in the concrete is equal to the strain in the steel. Using the mill certified elastic modulus of the strand the change in stress in the strand can be determined. This stress change represents the reduction in prestress due to creep, shrinkage and elastic shortening. Since relaxation of the strand occurs without a change in length, the relaxation must be added to determine the total loss. The AASHTO [2000] estimate of relaxation is used. The resulting effective prestress for the

two concretes are presented versus time in Figure 5B. The HESC and SCC maintain greater prestress than standard assumptions. In addition, the SCC exhibits less loss than the HESC over the first 75-days. Based on the trend of the measured response long term losses will remain above code estimates.

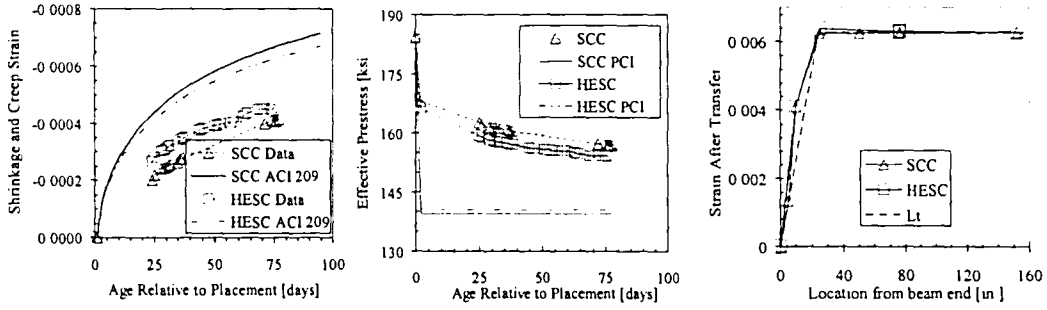

A) B) C)

Figure 5: Non-destructive properties

The PCI [1997] transfer length estimate (24.3-in.) is conservative when compared with the measured response in the SCC and HESC beams. The strain was measured in the beam along the strand during release of prestress. The strain was monitored during the entire release period. The change in strain of each gauge before and after release is used for calculation of transfer length. The strain is corrected to account for the existing strain in the strand and the vertical location where the strains were measured. The strain distribution after release of prestress is presented in Figure 5C. Both the SCC and HESC have comparable transfer properties of 15.7 and 15.8-in., respectively.

6.8.2. Ultimate Strength Performance

The full-scale bulb tee beams were tested to failure to examine shear, flexure and bond properties of the prestressed systems. A line load was applied in a monotonic manner at a section until a significant decrease in strength was observed. Beam displacement, surface strains, shear and flexural deformations, and end slip were recorded.

Table 6: Measured ultimate strengths									
Type	Config.	Age [days]	f'c [ksi]	fpe [ksi]	M_{max} [kip-in]	V_{max} [kip]	$\frac{M_{max}}{M_n}$	$\frac{V_{max}}{V_n}$	Failure mode
HESC	A	85	9696	156.0	44316	343.9	101%	75%	Compressive flexural failure
	B1	71	9183	154.1	44792	488.8	103%	107%	Web Shear
	B2	93	10037	155.2	19812	217.9	104%	52%	Tensile flexural failure
SCC	A	99	10330	151.5	44463	345.0	101%	76%	Compressive flexural failure
	B1	46	8930	159.9	44314	483.7	102%	106%	Web Shear
	B2	107	10720	150.8	19452	214.0	101%	51%	Tensile flexural failure

All beams exceeded their estimated capacities. The measured maximum moment and shear, M_{max} and V_{max}, are tabulated in Table 6. The age of the concrete at the day of test is noted along with the in-situ compressive concrete strengths and effective prestress. The PCI moment and shear, M_n and V_n, are computed using the actual material properties. The estimated ultimate strengths are computed using both the in-situ effective prestress and PCI estimates; the resulting variations are less than 1%. Tests A, B1, and B2 exceeded the measured flexural strengths by 1.0 to 4.0%. The shear capacity configuration (B1) exceeded the shear strength estimates by 6 to 7%.

The beam response conformed to an expected progression of failure. All HESC and SCC beams initiated with flexural cracking at the beam soffit directly under the applied load. Web shear cracking and progression of flexural cracks followed with increased loading in configuration A and B1. Spread of shear cracking progressed toward the near support where greater shear demand existed. Configuration A failed due to flexural failure initiated by compressive crushing of the top flange. Configuration B1 failed due to a shear failure of the web which progressed in an explosive manner through the section. Configuration B2, the reduced section, failed due to tensile fracture of bottom strands at the loaded section. A schematic of the damage associated with each test is presented in Figure 6.

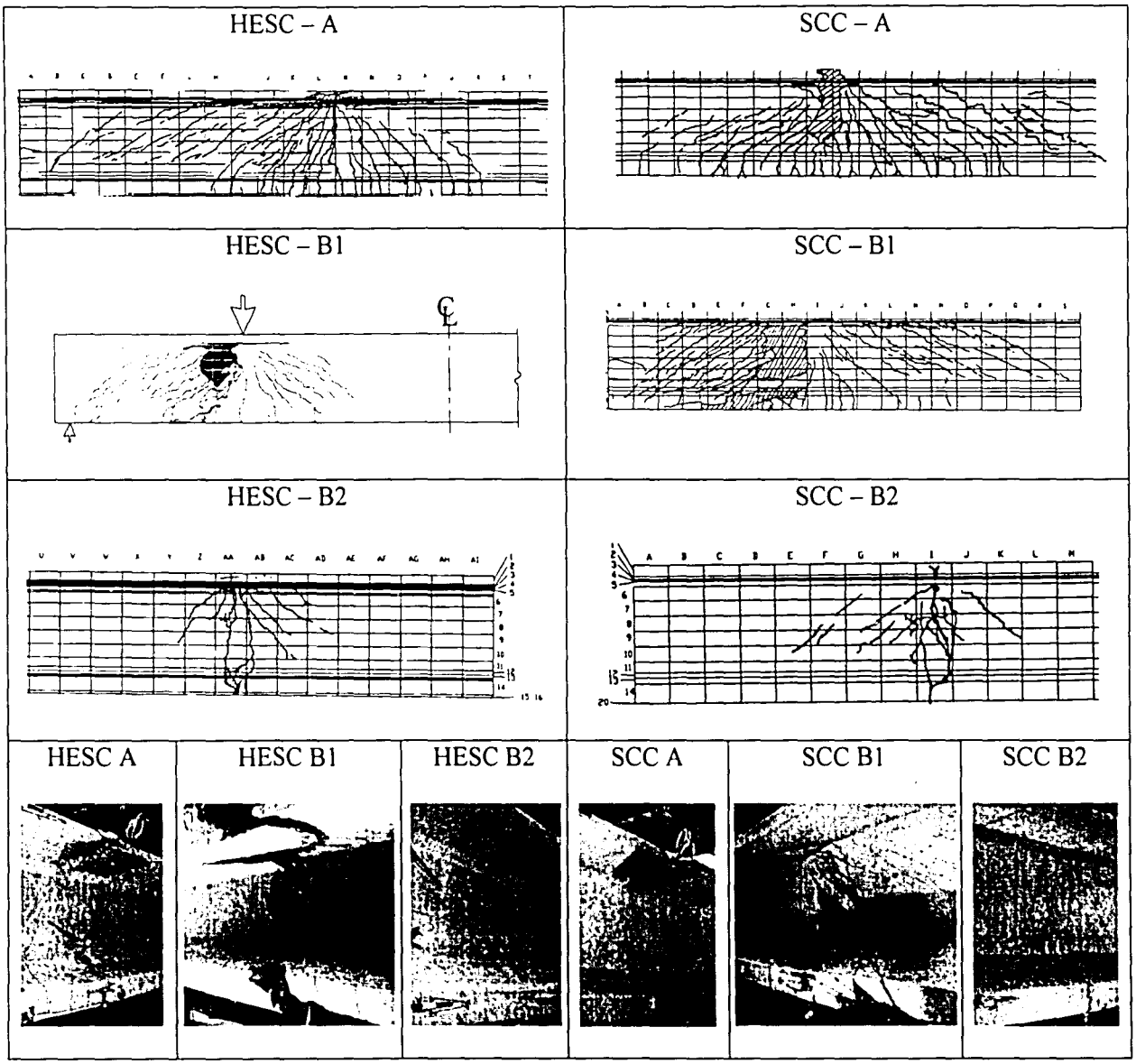

Figure 6: Specimen damage at failure

The moment resistances are consistent between the tests and between materials. The vertical beam deformation at the location of the applied load is plotted with respect to the moment and shear at the section Figure 7. All six load histories are compared on each graph. SCC has a consistently higher deformation capacity than that of the HESC. The limited deformability exhibited by configuration B1, in comparison to A, is due to the higher shear demand which resulted in a web failure prior to

significant yielding of the strand. The lower moment capacity and deformability of test B2 is due to the reduced cross-section and initial crack formation. These conditions resulted in a single flexural crack in B2 as compared to the distributed cracks observed A, compare Figure 6 A and B2.

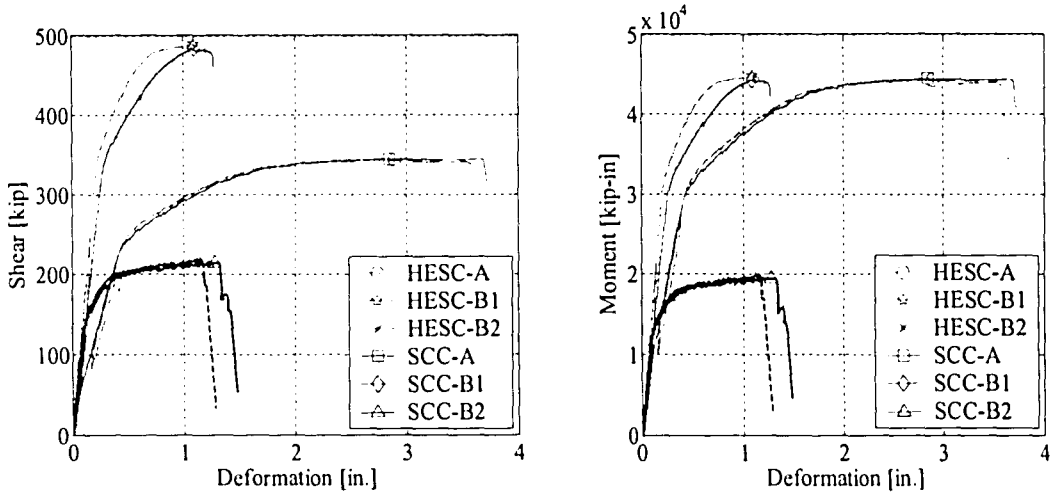

Figure 7: Moment and shear resistance

6.8.3. Strand Slip

Both the SCC and HESC were resistant to concrete to strand bond slip. Slip was monitored on both ends of the beam with instrumentation concentrated on side nearest the applied load. No slip was measured on any of the far end transducers, consequently only the near slip is discussed. Slip occurred in a non-symmetric manner. Some strands exhibited moderate slip while others, sometimes located adjacent to the slipping strand, exhibited none. The slip in all cases was minimal with a maximum value less than 0.05-inches.

The slip versus applied load for each test is presented in Figure 8. The global load versus deformation is presented to provide a reference to onset of slip. In general, slip coincided with global inelastic response. The level of slip was comparable between the two materials. The full span tests exhibited moderate slip. For these tests the full development length was provided however significant shear cracking formed. It could be argued that the slip was due to compatibility with the formation of

shear cracks. The most pronounced slip was observed in the short span tests on the SCC and HESC beams. In this configuration the embedment length was less than the required development length. In both the HESC and SCC, only a small portion of the strands exhibited measurable slip. In all cases the load was maintained with initiation of slip. Based on these results it is unlikely that the slip resulted in loss of flexural strength. The strands in the reduced section tests, where strands reached their fracture strength, no slip was measured. It can be concluded that the SCC and HESC provides adequate bond characteristics to prevent slip when using a full development length.

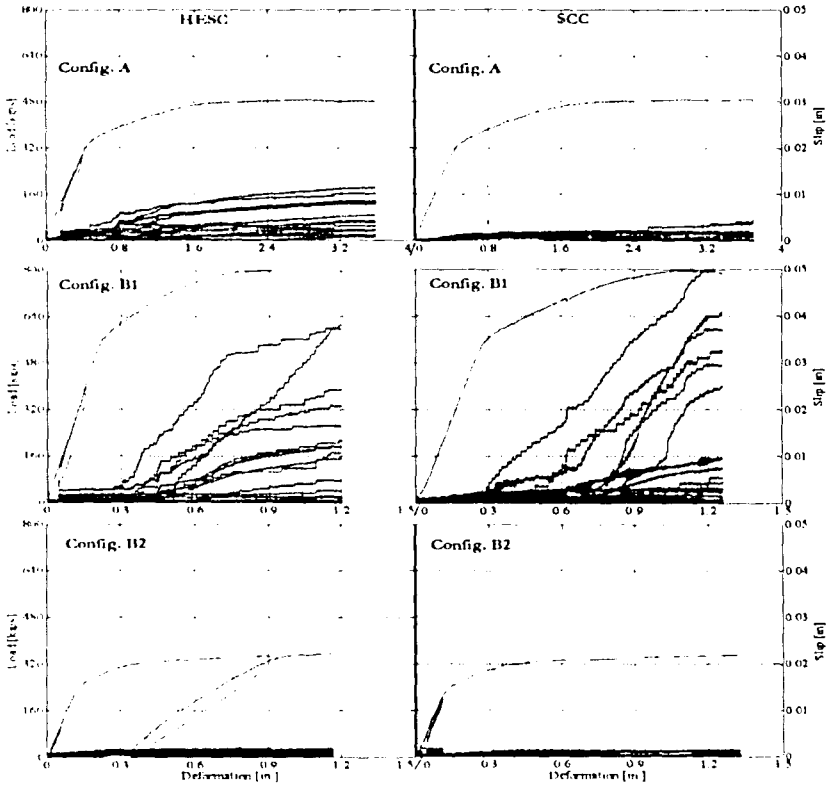

Figure 8: End slip of strand

6.9. CONCLUSIONS

An evaluation on the use of self consolidating concrete (SCC) for structural prestressed-precast bridge beams was conducted. The study examined the material in a plastic and hardened state and the performance when used in conventional bridge bulb tee beams. To provide a baseline, the response

was assessed relative to a conventional high early strength concrete (HESC) commonly used in precast bridge construction. The material is evaluated from a mechanical and durability standpoint, to assess if its use would provide an advantage over conventional concretes when used in structural bridge members. These goals were achieved through a series of material tests and ultimate load testing of full scale bulb tee beams. The following conclusions can be made from the research presented.

- Early strength gain properties were comparable to traditional high early strength concretes. The 5.2 hour and 6.3 hour setting times for HESC and SCC, respectively, are within a reasonable range for precast operations. The time of set can be accurately predicted with a power function.
- Elevated curing temperatures on the order of 140°F were used during the initial 24 hours to assist with rapid achievement of compressive strength. This resulted in a rapid leveling of strength followed by a an acceleration in strength gain after 56-days. The trends observed do not follow conventional ACI models for long-term strength gain.
- The tension capacities of the concretes are conservatively higher than ACI estimates. The direct tension capacity and modulus of rupture are comparable when normalized to the square root of the compressive strength. With the SCC having a marginally higher strength.
- Cylinder testing indicated that SCC has a lower elastic modulus than the HESC which contradicted in-situ testing. The measured camber and elastic shortening of the beams and surface strains measured during elastic loading indicated that the SCC had a higher in-situ modulus than the HESC.
- ACI 209 over-predicted the shrinkage characteristics of both the SCC and HESC. The ACI estimated creep coefficient, however, was under predicted for SCC. Consequently, the in-situ

creep and shrinkage in the prestressed bulb tee beams was consistently lower than estimates resulting in less prestress losses in the beams.

- Large block pullout tests of the strand resulted in an average bond capacity of only 84% of the accepted capacity. Nevertheless, under ultimate flexural loading of the beam no appreciable slip occurred in the strand.

- The length required for transfer of initial prestress is shorter than that expected from standard PCI formulations. This indicates that the concrete to strand bond properties are within code expectations. Long term monitoring of this trend should be conducted through additional research.

- The transfer length required for both the HESC and the SCC compare well with each other. This indicates that the SCC could be expected to provide strand to concrete bond properties similar to HESC.

- The losses measured in the beam sections are less than code estimations. Furthermore, the SCC exhibited less loss than the HESC. At 28 days the effective prestress measured in the SCC girder was 16% higher than the value that the PCI estimates. At 28 days the effective prestress measured in the HESC girder was 13% higher than the value that the PCI estimates.

- The SCC and HESC exceeded the nominal design strengths for all conventional beam failure modes. The design strengths were exceeded for a shear failure mode, flexural compression failure mode, and flexural tension failure mode. The beams achieved between 101%-104% of the predicted moment capacity and 106%-107% of the predicted shear capacity.

- Observed progression of damage was consistent between the SCC and HESC beams tested under the same conditions. The SCC in all cases provided greater ductility than the HESC.

- Measured end slip was observed on all but the reduced beam sections. Slip occurred in a non-symmetric manner about the section with slip on some stands and none on others. In all cases a minimal slip less than 0.05-in. was observed. Strand slip and inelastic deformation of the beam initiated at the same time. Load carrying capacity increased after slip initiated.
- Strand slip was observed in the beam with the full development length and the beam with the reduced development length. In the reduced section tests no slip occurred. It is the opinion of the authors that shear cracking resulted in end slip due to section compatibility. Furthermore after the onset of strand slip increase in shear and flexural strength was observed.

The research results indicate that the self consolidating concrete studied provides mechanical characteristics that outperform current recommendations. The material test results and accompanying full-scale beam tests indicate that SCC is a viable material for construction of prestressed bridge beam members. It is important to note that the research program was conducted on a particular mix design using proprietary admixtures. The conclusions drawn in the research are with respect to the mix studied. Alternate mixes should be investigated independently.

6.10. FUTURE WORK

While the presented research provides a comprehensive study of SCC for use in prestressed bridge beam construction further examination of a few topics is recommended to supplement this work.

1. The research was conducted on a particular SCC mix design. To properly assess the material, similar studies should be conducted on other SCC mix design based on different constituent proportions and admixtures.
2. Freeze thaw evaluation of the mixes should be conducted to assess the sensitivity to variations in AEA content and HRWR type on durability. This should be supplemented with hardened or plastic air void characterization tests to allow for correlation.

3. Long term chloride permeability tests should be conducted to examine the sensitivity to corrosion when using SCC and to allow correlation with rapid chloride permeability tests.

4. Fatigue tests should be conducted to assess the potential for bond loss in pre-cracked SCC beams subjected to repeated loading.

6.11. ACKNOWLEDGEMENT

The project was financed by Schuylkill Products Inc. and a grant from the Commonwealth of Pennsylvania, department of Community and Economic Development, through the Pennsylvania Infrastructure Technology Alliance (PITA) and through the support of, the Pennsylvania Department of Transportation, the Precast Association of Pennsylvania, and DeGussa Construction Chemicals. The researchers would like to thank Mark Hoover, Joe Nagle, Heinrich Bonstedt, Robert Horwhat, Serge Ter-Arakelov, and Bryan Spangler, and the staff at Schuylkill Products Inc. for their valuable contributions to this project.

6.12. REFERENCES

ACI Committee 209, "Prediction of Creep, Shrinkage, and Temperature Effects in Concrete Structures (ACI 209R-92)," American Concrete Institute, Farmington Hills, Mich., 1997, 47 pp.

ACI Committee 318, "Building Code Requirements for Reinforced Concrete (ACI 318-89) and Commentary (318R-89)," American Concrete Institute, Farmington Hills, Mich., 2005, 353 pp.

American Association of State Highway and Transportation Officials. "AASHTO LRFD Bridge Design Specifications," Washington, DC: May 2000.

ASTM International. A615, C39, C260, C494, C403, West Conshohocken, PA.

Commonwealth of Pennsylvania Department of Transportation, "Publication 408/2003 - Specifications," www.dot.state.pa.us, October 2004.

Daczko, J., A., "Stability of Self-Consolidating Concrete, Assumed or Ensured?," Conference Proceedings: First North American Conference on the Design and Use of Self-Consolidating Concrete, Master Builders, November 12-13, 2002.

Freyne, S.F., Russell, B.W., and Bush, T.D. Jr., "Heat Curing of High-Performance Concrete Containing Type III Cement," ACI Materials Journal, V.100, No.6, Nov.-Dec. 2003, p.449-454.

Geiseler, J., Kollo, H., and Lang, E., "Influence of Blast Furnace Cements on Durability of Concrete structures," ACI Materials Journal, V.92, No.3, May-June 1995, p.252-257.

Kosmatka, S.H. and Panarese, W.C., "Design and Control of Concrete Admixtures," Skokie, IL: Portland Cement Association, 1988.

Logan, D., R., 1997, "Acceptance Criteria for Bond Quality of Strand for Pretensioned Prestressed Concrete Applications," *PCI Journal*, V. 42 No.2, Mar-Apr., pp. 52-90.

Naito, C., Parent, G., Brunn, G., and Tate, T., "Comparative Performance of High Early Strength and Self Consolidating Concrete for Use in Precast Bridge Beam Construction," PITA Project PIT-457-04, ATLSS Report 05-03, Bethlehem, PA, June 2005.

PCI FAST Team, "Interim Guidelines for the Use of Self-Consolidating Concrete in Precast/Prestressed Concrete in Precast/Prestressed Concrete Institute Member Plants," TR-6-03, PCI, April 2003, pp.88.

Popovics, S., 1971, "Physical Aspects of the Setting Time of Portland Cement Concrete," Journal of Materials, JMLSA, Vol.6, No.1, March, pp.150-162.

Precast / Prestressed Concrete Institute. "Precast Prestressed Concrete Bridge Design Manual," Chicago: 1997.

7. PART 2: BOND STRENGTH EVALUATION TECHNIQUES PCI JOURNAL SUBMISSION

7.1. ABSTRACT

Successful use of prestressing in concrete members is dependent on the effective transfer of force between the concrete and the prestressing strand. The behavior of a prestressed beam under service loads is also influenced by the quality of this bond. While the general bond mechanisms involved in the transfer operation are known, few studies have been conducted with the goal of quantifying the mechanisms' contributions to the total bond strength. Consequently, potential bond problems are difficult to identify before they are observed. Due to recent developments in the prestressing industry, a systematic examination of strand-concrete bond is particularly relevant.

Four major bond mechanisms contribute to total bond strength: adhesion at the strand-concrete interface, mechanical interlock due to axial bearing forces on helical strand, frictional forces augmented by radial stresses in the strand after release of prestress, and frictional forces augmented by surface friction at the strand-concrete interface. A research program of multiple tests that incorporate different combinations of these bond mechanisms is conducted to satisfy three objectives: 1) to compare the bond characteristics of seven wire prestressing strand to high early strength concrete (HESC) and SCC, 2) to develop a simplified evaluation method to accurately assess bond characteristics in prestressing applications. Test results indicated that SCC and HESC are comparable for use in prestressing applications, and that a new test, the direct tension pullout test, proved an efficient means of evaluating the bond capacity of a prestressed member. In addition, the new test provided a means of predicting development lengths in full size concrete beams, and corroborated

widely accepted evidence that the ACI transfer and development length prediction equations provide conservative results.

7.2. INTRODUCTION

Successful use of prestressing in concrete members is dependent on the effective transfer of force between the concrete and the prestressing strand. While the general bond mechanisms involved in the transfer operation are known, few studies have been conducted with the goal of quantifying the mechanisms' contributions to the total bond strength. Consequently, potential bond problems are difficult to identify before they are observed. Various bond test methods have been developed with the goal of pre-qualifying the *strand* prior to shipment from the supplier; however, these methods do not necessarily validate the use of the strand in its intended application.

Simple, easy-to-conduct methods that validate strand-concrete bond on prestressed specimens are not in widespread use. Strand can also be used in a variety of concrete types such as normal strength concrete, high early strength concretes, or self consolidating concrete. The variation of concrete strength, cement type, quality of consolidation, aggregate gradation, strand surface area, and prestressing level all play a vital role in the bond transfer process. To achieve accurate quantification of strand-concrete bond capacity, each of these issues must be examined systematically. Also, the use of self-consolidating concrete (SCC) in the prestressed/precast industry has grown, despite a lack of literature addressing the product's bonding characteristics to prestressing strand. These two developments provide an opportunity for a testing program that incorporates existing and new tests to explore both the bond mechanics of prestressing strand and the bond characteristics of SCC.

7.3. RESEARCH OBJECTIVES

The research program is guided by two main objectives:

1) Compare the bond characteristics of seven wire prestressing strand to high early strength concrete (HESC) and SCC.
2) Develop a simplified evaluation method to accurately assess bond characteristics in prestressing applications.

Current tests used by precast/prestressed manufacturers are typically derivatives of the large block pullout test summarized by Logan [1997]. While this test provides a qualitative evaluation of bond strength of one strand or concrete type relative to another, it only partially reproduces the actual strand-concrete bond conditions in a prestressed product. Because the strands are never stressed, certain bond mechanisms present in the pullout block may not be present in an actual prestressed element. At the same time, though flexural beam tests [Hanson and Kaar 1959] accurately mimic real conditions by testing an actual prestressed beam, prescast/prestressed manufacturers may not have the specialized equipment and instrumentation required for a successful test readily available. A new test that combines the cost effectiveness and simplicity of pullout blocks with the realistic prestressed conditions of the flexural beam test style is proposed herein.

7.4. DIFFERENT TYPES OF TESTS FOR BOND STRENGTH

Method	Bond mechanisms present			
	Adhesion	Mechanical Interlock	Friction – Radial Stresses	Friction – Surface Rough.
Flexural beam test	✓	✓	✓	✓
Bond strength assessment through end slip		✓	✓	✓
Large block pullout test	✓	✓		✓
Abrishami & Mitchell transfer and flexural bond tests	✓	✓	~	✓
Cousins, Badeaux, & Moustafa "push-off" method	✓	✓	~	✓
Rose and Russell "tensioned pullout" method	✓	✓	~	✓
NASP Tests	✓	✓		✓
Peterman "pass/fail" tests	✓	✓	✓	✓

Direct tension pullout tests	~	✓	✓	✓

Table 7 Bond mechinisms present in current tests.

7.4.1. Pro's and Con's of different tests

Flexural beam test

Pro: Specimen is an actual prestressed beam. This test incorporates full range of bond mechanisms.

Con: Difficult to conduct without special equipment, gauges, and data acquisition systems. Fabrication may be complicated by use of shear reinforcement and strain gauges, which may in themselves affect results.

Bond strength assessment through end slip

Pro: Incorporates all mechanisms associated with prestressing. Strands are embedded in horizontal orientation similar to actual prestressed member.

Con: Only one data point from each test. Does not give indication of bond performance at strand stresses higher than effective prestress

Large block pullout test

Pro: Specimens are easy to fabricate and test.

Con: Does not incorporate bond mechanisms associated with prestressing.

Strands embedded in vertical orient

Abrishami & Mitchell transfer and flexural bond tests

Pro: Incorporates all mechanisms associated with prestressing. Strands are embedded in horizontal orientation similar to actual prestressed member.

Con: Short embedment length, radial stress mechanism only partially developed. This test may not fully mimic a prestressed member. This test is difficult to repeat and it requires a special apparatus

. **Cousins, Badeaux, & Moustafa "push-off" method**

Pro: Incorporates all mechanisms associated with prestressing. Strands are embedded in horizontal orientation similar to actual prestressed member.

Con: Short embedment length, radial stress mechanism only partially developed. This test may not fully mimic a prestressed member. This test is difficult to repeat and it requires a special apparatus

Rose and Russell "tensioned pullout" method

Pro: Incorporates all mechanisms associated with prestressing. Strands are embedded in horizontal orientation similar to actual prestressed member.

Con: Short embedment length, radial stress mechanism only partially developed. This test may not fully mimic a prestressed member. This test is difficult to repeat and it requires a special apparatus

NASP Tests

Pro: Used for strand evaluation purposes.

Con: Only applicable to strand quality comparisons.

Peterman "pass/fail" tests

Pro: Project currently underway.

Con: Project currently underway.

Direct tension pullout tests

Pro: Easy to fabricate and conduct. No special apparatus required. This test incorporates actual bond mechanisms.

Con: Requires space in prestressing bed for fabrication. This is a destructive test.

7.5. EXPERIMENTAL PROGRAM

The experimental program uses common bond test methods, derivations of common test methods, and a new test method to fulfill the research objectives of addressing a lack of information over SCC bonding properties, developing a new test method, and quantifying individual bond mechanisms.

7.6. EXPERIMENTAL PROCEDURES

7.6.1. Large Block Pullout Test

The large block pullout test provides a basis for comparison of DTPT results and a means to study the mechanical interlock, chemical adhesion, and surface roughness bond mechanisms inherent in an unstressed specimen. The test is based on procedures for the Large Block Pullout Test outlined by Logan [1997]. In the test, unstressed strand specimens are pulled out of a large concrete block and load-slip relationships are recorded. The test provides a direct measure of the bond capacity of unstressed strand. A diagram of the test setup is shown in Figure 9.

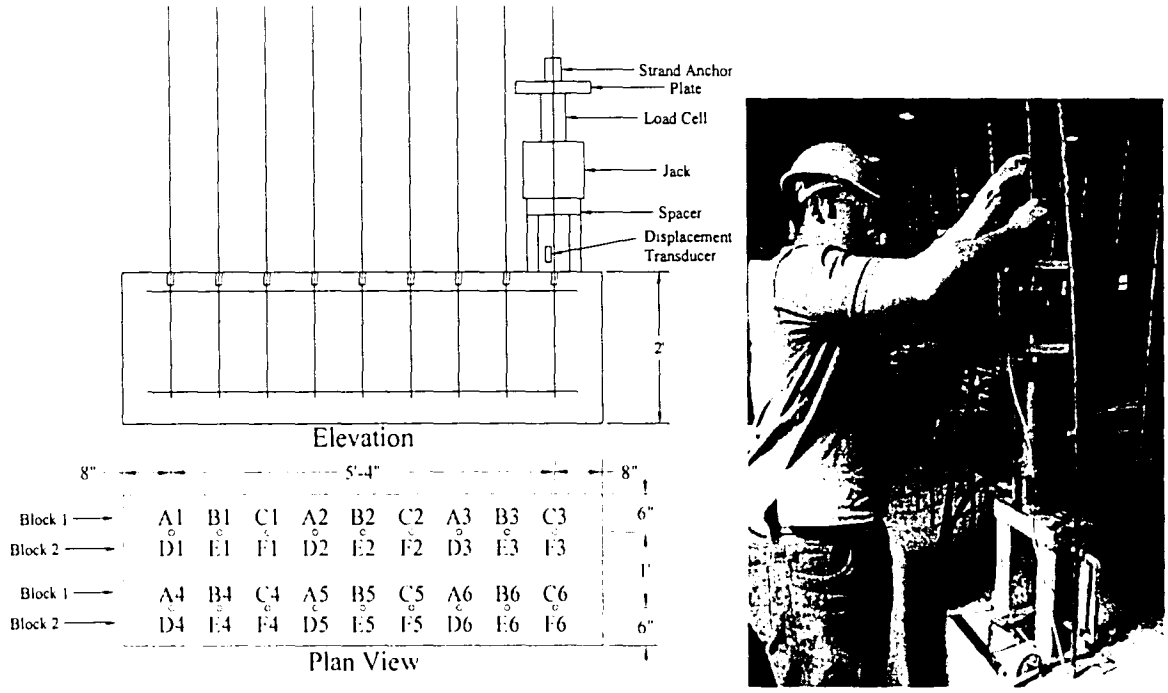

Figure 9. Large Block Pullout test

7.6.2. Flexural Beam Test

The flexural beam test was used to provide a direct comparison for DTPT performance and to examine the bond mechanism performance in an actual prestressed beam. The test, pictured in Figure 10, is in part based on the original flexural bond tests conducted by Hanson and Kaar [1959]. Simply supported, single-strand prestressed concrete beams were subjected to an increasing point load at midspan. The beams had a rectangular, 6.5" x 12" cross section. A compression machine was used to support the specimen and apply a point load at midspan. A diagram of the test setup is shown in Figure 10.

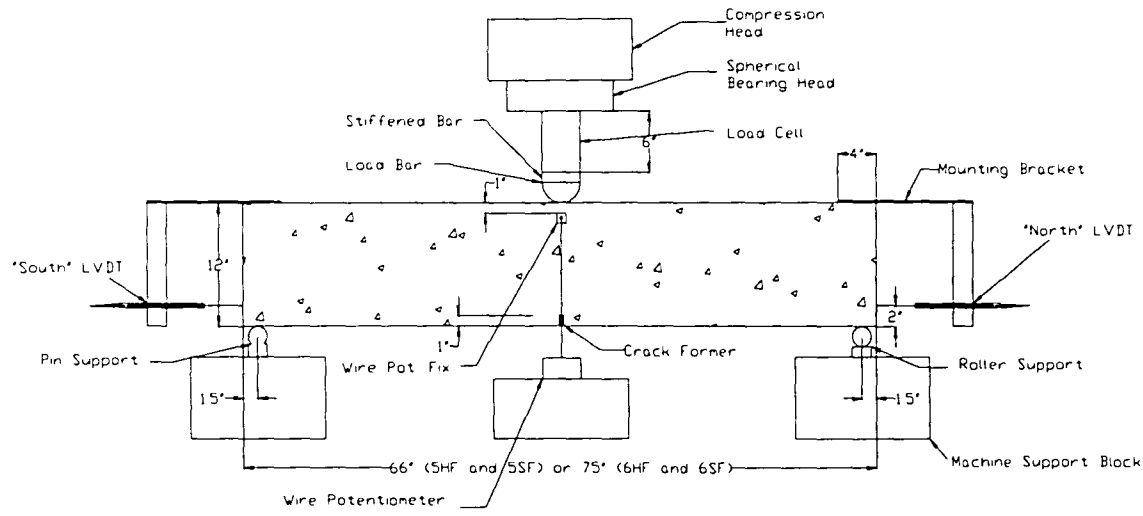

Figure 10. Flexural Beam Test

7.6.3. Direct Tension Pullout Test

The direct tension pullout test (DTPT) was conducted to evaluate the ability of a new test for bond strength to accurately depict the bond performance of various prestressing materials under the full distribution of bond mechanisms associated with prestressing. The DTPT, pictured in Figure 11, combines the realistic bond mechanisms of a flexural beam test with the ease of operation of a direct pullout test. DTPT specimens are short beams of rectangular 6.5" x 12" cross section that are prestressed using a single seven-wire strand. The prestressing steel runs through the centroid of the cross-section so that concrete cover around the strand can be maximized. Since the beams are only loaded axially, no shear reinforcement is included. A typical specimen diagram is pictured in Figure 11. Specimens were fabricated so that 40" of strand protrudes from the end of the beam

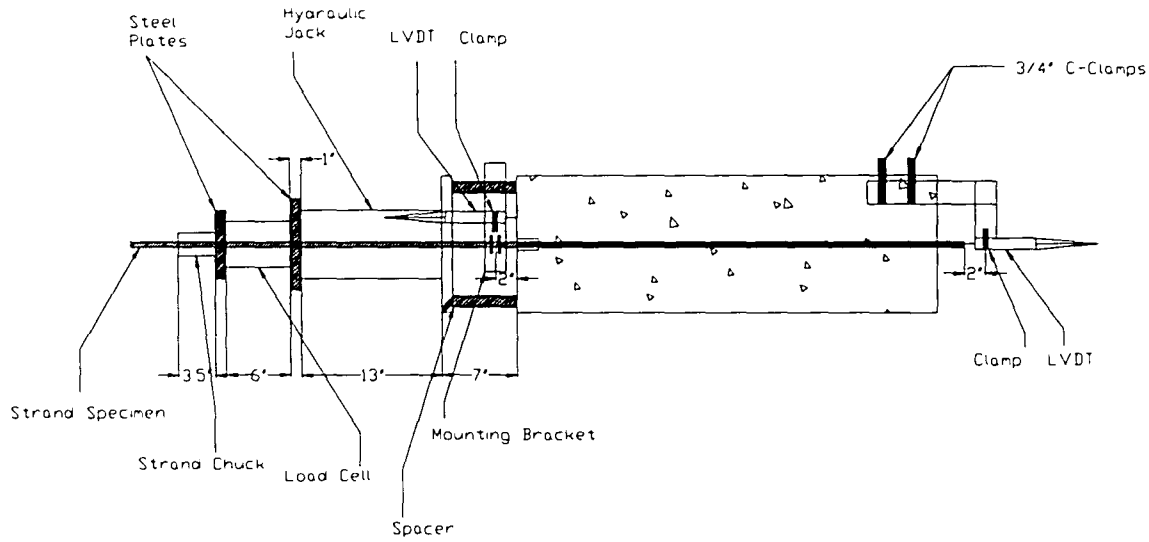

Figure 11. Direct Tension Pullout Test

7.7. TEST MATRIX

Method	Bond mechanisms present			
	Adhesion	Mechanical Interlock	Friction – Radial Stresses	Friction – Surface Rough.
Large Block Pullout Test – Strand	✓	✓		✓
Large Block Pullout Test – Wire	✓			✓
Flexural Beam Test	✓	✓	✓	✓
Direct Tension Pullout Test	~	✓	✓	✓

Table 8. Tests conducted in this research program

7.8. MATERIAL PROPERTIES

7.8.1. Mix Design

Concrete Mix	Average of Batches	
Material Type	HESC	SCC
Total Cement [lb/yd^3 (kg/m^3)]	**750(445)**	**849(504)**
Slag Cement [%]	**34**	25
Fine Aggregate SSD [lb/yd^3 (kg/m^3)]	**1172 (695)**	**1283(761)**
Coarse Aggregate #67 SSD [lb/yd^3 (kg/m^3)]	**1383(820)**	0
Coarse Aggregate #8 SSD [lb/yd^3 (kg/m^3)]	**552(327)**	**1651(979)**
Water / Cement Ratio	0.34	0.32
High Range Water Reducer [oz/yd^3 (ml/m^3)]	60.0(2320)	136.2(5270)
Retarding Admixture [oz/yd^3 (ml/m^3)]	4.0(154)	0
Air Entrainment Admixture (AEA) [oz/yd^3 (ml/m^3)]	2.4(93)	2.0(76)
Viscosity Modifying Admixture [oz/yd^3 (ml/m^3)]	0	16.0(620)
Coarse Aggregate Volume [%]	39	34
Target Air Content [%]	NA	NA
Target Slump / Spread [in. (cm)]	NA	NA

Table 9. Mix Design

7.8.2. Concrete Properties

Concrete Material Properties by Specimen Series						
Concrete Group	Affected Series	Cast Date	f'_c (28 day) [psi]	E_c (28 day)* [ksi]	f'_r (28 day)** [psi]	f'_t*** [psi]
5H	5HMS, 5HMW, 5HF, 5HA	10/13/2004	7485	5287	951.7	509.5
5S	5SMS, 5SMW, 5SF, 5SA	10/13/2004	7836	4658	973.7	560.5
6H	6HMS, 6HMW, 6HF, 6HA	10/18/2004	6707	4790	900.9	462.5
6S	6SMS, 6SMW, 6SF, 6SA	10/18/2004	7809	4481	972.1	527.9

**$f'_r = 11(f'_c)^{1/2}$ for these batches according to tests conducted by Naito and Parent 2005

***f'_t is 28-day value for 5-groups and 42-day value for 6-groups.

Table 10: Concrete material properties by specimen series

It is important to note that for this research program, SCC exhibits higher 28-day compressive strengths than HESC, as shown in Table 10. Consequently, application of the f'_r equation derived

from Parent and Naito's [2005] experimental results for identical mixes shows that SCC has a higher modulus of rupture than HESC. SCC's higher compressive strength (f'_c) and splitting tension (f'_t) may directly affect its bonding performance, particularly in bond models that relate bond strength to these properties. Though splitting tension f'_t affects the pure tensile capacity of bond, the affect of $\sqrt{f'_c}$ on bond will be considered because the f'_t data for the test series are inconsistent. Contrary to the compressive strength and splitting tension trends, HESC has a higher experimentally determined Young's modulus, indicating that HESC is slightly stiffer than SCC.

7.8.3. Strand Properties

The strand used in the project was produced by both the American Spring Wire Company (ASW) in Ohio and Insteel. ASW produced the 0.5" special strand, and Insteel produced the 0.6" strand. The low relaxation 270ksi strand was used in all facets of the project. Two lots of strand were used in the project—one 0.5" special, the other 0.6" strand. Strand was placed in specimens in the "as-received" surface condition, and was only submitted to light wipe down to remove dirt affixed to the strand. The mechanical properties are presented in Table 11.

Strand Properties: 270k Low Relaxation Strand							
Designation	Modulus [ksi]	Area [sq. in]	Yield [ksi]	Yield Strain	Ultimate [ksi]	Fracture Strain	2nd Modulus [ksi]
0.5" special strand (ASW)	29080	0.1639	256.7	0.010175	280.3	0.085400	314.2
0.6" strand (Insteel)	29000	0.2172	262.2	0.010000	286.1	0.067000	419.1

Table 11: 270k low relaxation strand properties

7.9. TEST RESULTS

7.9.1. Large block pullout test

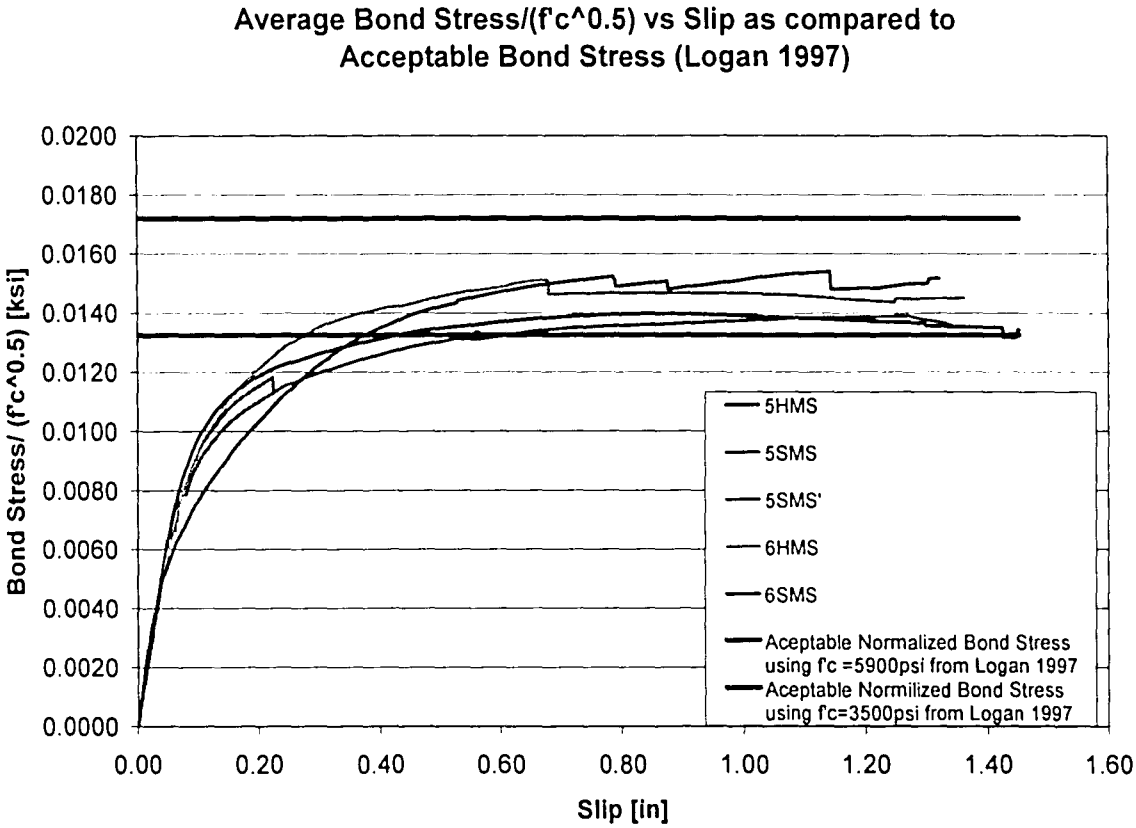

Figure 12 Normalized Average Bond Stress compared to Acceptable Bond Stress (Logan 1996)

$$\mu = \frac{f_s * A_s}{l * SA} \qquad \text{Equation 1}$$

Logan's 1997 PCI journal stated that, "the following benchmark is recommended as the minimum acceptable pull-out capacity: Average pull-out load = 36 kips" The 36 kip pull-out load can be converted to bond stress using Equation 1. The acceptable bond stress can then be compared to the bond stress calculated from the large block pull-out test. However, the acceptable pull-out load discussed in Logan's 1997 PCI journal was for concrete that had strength of 3900psi – 5900psi. The concrete in our test had a range in strength of approximately 6700psi – 7800psi. Therefore the pullout loads in this research were consistently higher than Logan's acceptable value. Figure 12 was

developed by dividing the calculated bond stress by the corresponding square root of f'c for each test. This normalizes the bond stress so that the bond stress in independent of concrete strength.

$$\frac{\text{Acceptable bond stress}}{\sqrt{f'c}} = \frac{36kip}{18in * 1.966in * \sqrt{5900psi}} = 0.01324\frac{ksi}{\sqrt{psi}}$$

As can be seen in Figure 12, for every case, the average bond stress calculated from the large block pull-out test exceeds the acceptable bond stress calculated using 5900psi concrete. This confirms that the bonding properties between the strand and the concrete in this research program are acceptable for use in prestressed applications.

7.9.2. Flexural Beam Test

Because they accurately mimic the bond behavior of an actual prestressed beam, flexural beam tests are an essential part of the investigation of the effects of different prestressing materials on bond performance. In addition to providing a platform on which different material combinations can be tested, the test also provides a realistic basis for comparing the advantages and disadvantages of different testing methods. If it were not for the tests' complexity in instrumentation, apparatus, and data analysis requirements, the flexural beam test would make an excellent tool for gauging the reliability of prestressing products.

Unlike the pullout tests, data produced from the flexural beam tests relates applied load at midspan to end slip, rather than pullout force to slip. A section analysis is therefore used to determine the stress in the strand at midspan for every increment of load applied to the beam (Nawy). Steel stress at midspan under applied load is modeled as a pullout force, and an equivalent average uniform bond stress is also calculated. This pullout force is applied to one half of the total embedment length of the beam. The "half-beam" considered, therefore, resembles a DTPT specimen. However, while the initial pullout force for the large block and DTPT specimens is zero, the initial pullout force modeled for the flexural beam specimen was equal to the effective prestress of the strand. In addition, DTPT

specimens feature LVDTs at both the "live" and "dead" ends, while flexural beam specimens only have an LVDT at the "dead" end. Though each flexural beam test provides two sets of data (for each "half-beam") only the side that exhibited the first (and, typically, most) end slip under applied loading was used.

It is important to note that specimens that fail by strand rupture (typically, 0.5" strand specimens) exhibit a maximum slip of only 0.05" – 0.075", smaller than those of specimens that fail by concrete crushing (typically > 0.1"), and much smaller than slips observed in the pullout block tests. Such a minimal slip for fracture specimens indicates that a full development zone is "activated" with only a small displacement, thus corroborating other research discussed in the background and theory chapter.

Specimens that failed by strand rupture exhibited bond strengths that were greater than the ultimate tensile capacity of the strand. This suggests that full development was achieved within these specimens. Development lengths predicted using Equation 1, however, are much longer than the space available within the "half-beam" section, as shown in Table 12. "Observed" development lengths are calculated for each specimen by considering a condition that fulfills static equilibrium:

$$f_s \cdot A_s = l \cdot \mu \cdot SA \qquad \text{Equation 2}$$

Where f_s = the stress in the strand [ksi], A_s = the strand area [in^2], l = the length of strand-concrete bond counterbalancing the force [in], μ = the bond stress at the strand-concrete bond [ksi], and SA = the surface area of the strand in terms of unit length [in^2/in]. Since the strand cannot experience any stress higher than f_{pu}, the ultimate tensile capacity of the strand, and because μ is maximum at the maximum sustainable force (in this case, ultimate capacity), the relationship may be amended as follows:

$$f_{pu} \cdot A_s = l_d \cdot \mu_{max} \cdot SA \qquad \text{Equation 3}$$

Where f_{pu} = the ultimate tensile capacity of the strand [ksi], μ_{max} = the maximum bond strength at the strand-concrete interface, and l_d = the development length of the strand [in]. The equation may be used to isolate a conservative value of l_d and thereby determine what length of strand is needed, for a given quality of bond, to resist a pullout force ($f_{pu}A_s$) that equals the ultimate strength of the strand. Development lengths calculated using this equation are presented in Table 12.

		Flexural Test	Based on	ACI
		Development	f_{pe} Actual	Vs.
Series	μ_{max}	Length	ACI (l_d)	Actual
5HF1	**0.770**	**30.36**	**76.14**	**2.51**
5HF2	**0.761**	**30.70**	**76.14**	**2.48**
5HF3	**0.764**	**30.59**	**76.14**	**2.49**
5SF1	**0.762**	**30.69**	**73.85**	**2.41**
5SF2	**0.771**	**30.32**	**73.85**	**2.44**
5SF3	**0.722**	**32.36**	**73.85**	**2.28**
6HF1	0.773	34.52	89.92	2.60
6HF2	0.773	34.50	89.92	2.61
6HF3	0.662	40.28	89.92	2.23
6SF1	**0.772**	**34.55**	**92.68**	**2.68**
6SF2	**0.722**	**36.94**	**92.68**	**2.51**
6SF3	0.770	34.63	92.68	2.68
Average	0.752			2.49

Table 12: Comparison of predicted ACI l_d to l_d calculated in Flexural Tests.

NOTE: **Bold** specimens failed by strand fracture, indicating l_d was activated.

7.9.3. Current AISC Transfer and Development Length Equations

$$l_d = \left(\frac{f_{pe}}{3}\right) d_b + (f_{ps} - f_{pe}) d_b \qquad \text{[ACI 318 §12.9.1]} \qquad \text{Equation 4}$$

$$l_t = (f_{pe}/3)d_b \qquad \text{Equation 5}$$

In Table 12, observed development lengths were compared to the theoretical development length values predicted using the ACI code and both predicted and observed values of effective prestress, f_{pe}. As expected from observed flexural beam performance, the average development length for the flexural beam specimens is much smaller than the development length predicted by the ACI code equation. For the specimens considered, therefore, the ACI code equation is found to apply a factor of safety of approximately 2.5 to the actual development length. Specimens that experienced strand fracture had strand embedments comparable to the embedment length of the strand. Specimens that experienced concrete compression failure had strand embedments that were shorter than the calculated embedment length—thus experiencing bond failure before strand fracture could occur. Both SCC and HESC specimens had comparable observed development lengths, indicating a consistent bond performance between materials.

It is important to note that the maximum average uniform bond stress (μ_{max}) recorded represents a lower value of flexural bond strength than that actually present in a prestressed member. In typical prestressed beams, the full development length is activated with minimal strand slip at the beam ends (Naito and Parent 2005). Under these conditions, the transfer zone retains its full integrity and is not undermined by progressive destruction of bond—the flexural bond zone is distinct from the transfer bond zone. Short specimens, however, exhibit significant end slip before strand fracture, indicating that the extra bond strength was "activated" by a relative strand-concrete slip (i.e. mechanical interlock and surface roughness mechanisms) rather than extra embedment length. In these cases, the flexural bond zone and the transfer bond zone are forced to overlap. Because the flexural bond length for short specimens impinges on the transfer zone (which has suffered destroyed adhesion bond at prestress release), the maximum bond stress recorded for flexural beam specimens represents a lower bound on the actual flexural bond resistance that may occur in a full size prestressed member.

7.9.4. Direct Tensioned Pullout Tests

The direct tension pullout test (DTPT) is an approach to testing that resembles a hybrid between the flexural beam test and the large block pullout test. As previously discussed, the DTPT combines the realistic bond mechanism distribution found in the flexural beam test with the ease of use and repeatability of the large block pullout test. It is important to note that though specimens were designed to be only one ACI transfer length long, full transfer of prestress likely occurs because 1) The ACI equation for development length was found to conservatively predict development lengths 2.5 times the actual length, 2) The stress-slip curves developed from the DTPT specimens closely resembled those of the flexural beam specimens, and 3) Hanson and Kaar (1959) achieved full transfer of prestress with specimens of similar length. Though comparison of the relative performance of different prestressing materials in DTPT specimens serves to fulfill the first objective of the research program (explore the suitability of SCC), results that are found to be similar to those of other tests—particularly the flexural beam test—justifies the use of the DTPT as a suitable testing method.

7.10. DIRECT TENSION PULLOUT TEST AND FLEXURAL BEAM TEST COMPARISON

Because no other test more closely mimics the actual bond conditions in a prestressed beam, the flexural beam test serves as the benchmark by which the DTPT is rated. Two direct relationships exist between the DTPT and the flexural beam test that incorporate the aforementioned differences in specimen properties. These relationships are: 1) a direct mathematical relationship between the curves, 2) comparison of development lengths calculated from test results.

Discretizing the flexural beam Bond Stress-slip curves and DTPT load-slip curves into equal intervals yields the curves shown in Figure 13. The figure indicates that 5HF and 5SF specimens exhibit initial slip at a bond stress 1.6 times that of the initial bond slip of the dead end LVDT on the 5HA and 5SA

tests. Similarly, 6HF and 6SF specimens exhibit initial slip at a bond stress of approximately 1.2 times that of the corresponding DTPT tests. The curve appears to trend towards a value of 1 at larger slips, indicating that at high values of slip, average uniform bond stress is similar between the DTPT and flexural beam specimens. This conclusion corroborates the theory that regardless of initial distribution of bond mechanisms, large dislocations of the strand eventually "grind down" particles contributing to post-slip mechanical interlock, and only surface friction—identical in both test types—remains.

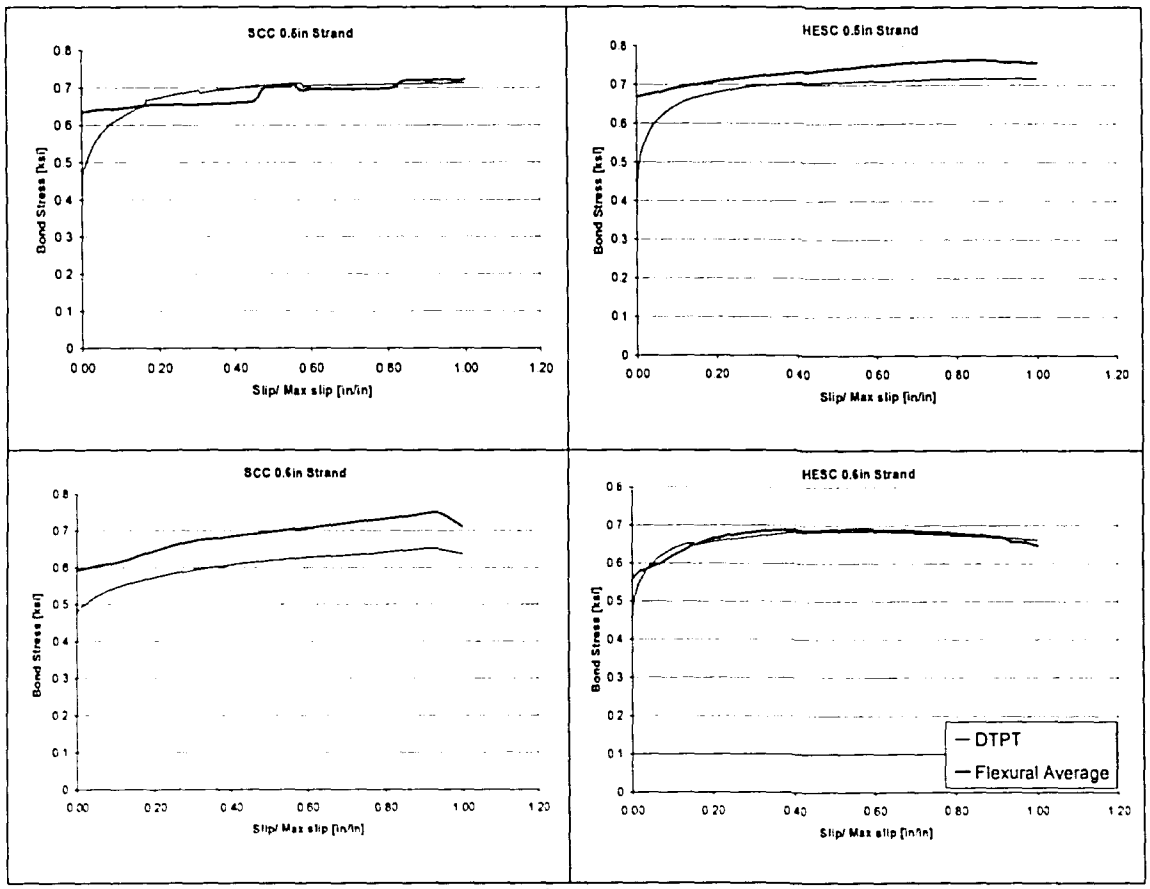

Figure 13: Comparison of flexural beam and DTPT Bond Stress

Figure 13 suggests a direct relationship between the bond stress-slip curves of the flexural beam specimens and the direct tension pullout specimens, particularly for large slip values.

In addition to correlation of the overall bond stress-slip curves, correlation also exists between development length results based on for DTPT and flexural beam specimens. Development lengths for DTPT specimens were determined using the same method that was used for the flexural beam specimens. Equation 3 was used to relate values for maximum average uniform bond stress to required development length for each DTPT specimen, presented in Table 13. Bolded specimens failed by fracture, others failed by general bond slip.

			*[in^2/in for strand]	DTPT Development Length	A Series Maximum Available
Specimen	**μ_{max} [ksi]**	**$f_{pu}A_s$**	**SA***	**l_d [in]**	**l_d**
5HA1	0.715	45.956	1.966	32.688	32
5HA2	**0.719**	**45.956**	**1.966**	**32.502**	**32**
5SA1	**0.712**	**45.956**	**1.966**	**32.839**	**32**
5SA2	**0.708**	**45.956**	**1.966**	**33.005**	**32**
5SA3	0.607	45.956	1.966	38.516	32
5SA4	**0.720**	**45.956**	**1.966**	**32.456**	**32**
6HA1	0.688	62.14	2.329	38.773	36.5
6HA2	0.682	62.14	2.329	39.122	36.5
6HA3	**0.671**	**62.14**	**2.329**	**39.751**	**36.5**
6SA2	**0.676**	**62.14**	**2.329**	**39.479**	**36.5**
6SA3	**0.680**	**62.14**	**2.329**	**39.257**	**36.5**

Table 13: Development lengths determined from DTPT tests, by specimen

Table 14 compares development length results for flexural beam and DTPT series of the same strand type and material type. The increase in DTPT development length over flexural beam development length corresponds to the lower observed bond stresses on the DTPT curves. The higher maximum bond stresses inherent in the flexural beam tests lead to lower development lengths. The relationship between the flexural beam specimens and the DTPT specimens already suggested by the load-slip curves is further corroborated in Table 14. Variations in percent differences are likely caused by the

different prestressing materials' responses to the small variations in bond mechanisms between the DTPT and flexural beam tests. Overall results, however, reiterate the trend of fairly consistent, higher maximum average uniform bond stresses in the flexural beam specimens.

Strand	Material	DTPT series l_d [in]	Flex Beam series l_d [in]	Percent Difference
5	H	32.595	30.55	6.7%
5	S	34.204	31.13	9.9%
6	H	39.215	36.44	7.6%
6	S	39.368	35.38	11.3%

Table 14: Comparison of Flexural Beam and DTPT development lengths

Figure 13 and Table 14 demonstrate the relationship between flexural beam test results and DTPT results. Because it provides results consistent to a generally accepted test for bond strength, the DTPT may be considered a viable means of evaluating the quality of bond in prestressing applications. In addition, the test may be used to determine the absolute magnitude of maximum average uniform bond strength in a full size prestressed member, should the conversion factors in Figure 13 and Table 14 be considered.

7.11. END SLIP AT PRESTRESS RELEASE MEASUREMENTS

The measurement of end slips immediately after the release of prestress provides an indication of the transfer bond quality of the strand-concrete interface—particularly in the relative sense. Such a relationship was previously defined in the theory and background section. Table 15 contains end slip comparisons for different materials based on average series values. Table 15 contains several specimen series of different strand type and embedment length that were not subject to pullout or flexural beam tests, including 5HC, 5HB, 5SC, 5SB, 6HB, and 6SB. Averages for each series were compared, and an average value for those comparisons was used to summarize the relationships. On average, 0.5" special strand specimens made of SCC exhibited 6.0% less end slip than their HESC

counterparts. Similarly, 0.6" strand specimens made of SCC experienced 14.4% less slip than their HESC counterparts. The smaller slips indicate higher transfer bond strength.

Series	Average Endslip	Type	S vs. H	0.5"sp vs. 0.6"	Average
5HF	0.086	5F	-9.10%		
5HC	0.073	5C	-18.20%		
5HB	0.060	5B	11.10%		
5HA	0.080	5A	-7.80%		-6.00%
5SF	0.078	6F	-27.80%		
5SC	0.060	6B	-8.80%		
5SB	0.067	6A	-6.70%		
5SA	0.074				-14.43%
6HF	0.075	HF		-12.70%	
6HB	0.113	HB		88.90%	
6HA	0.100	HA		25.00%	33.73%
6SF	0.054	SF		-30.70%	
6SB	0.103	SB		55.00%	
6SA	0.093	SA		26.60%	16.97%

Table 15 Comparison of end slips after release by specimen series

7.12. CONCLUSIONS

7.12.1. Suitability of SCC in prestressing applications

Based on the above results and discussion, SCC was determined to be a viable product for use in prestressed concrete applications. Summary conclusions are presented below:

- The SCC mixture used was found to sustain maximum bond stresses approximately equal to or greater than HESC.
- When bond responses are normalized to the 28-day $\sqrt{f'_c}$ for the concrete batches, HESC was found to outperform SCC in terms of maximum sustainable bond stress in nearly all cases.
- SCC's non-normalized performance improvements may be influenced by its ability to achieve higher 28-day compressive and tensile strengths than HESC.

7.12.2. Suitability of the Direct Tension Pullout test as a reliable method for bond stress evaluation

Based on the above results and discussion, the DTPT was found to be reliable method for evaluating bond strength capacity in a full-sized prestressed member. Summary conclusions are presented below:

- Of all test methods in the discussed in the program, the flexural beam test was found to provide the most realistic evaluation of bond capacity in a full-sized prestressed beam.
- The DTPT test specimens were found to have bond stress distributions similar to that of a flexural beam specimen.
- Close correlation between dead end load-slip curves of DTPT tests and flexural beam tests indicated that the DTPT provides a bond strength evaluation consistent with, though not identical to, that provided by the flexural beam test.
- Development lengths of DTPT specimens were found to correlate to those of flexural beam specimens consistent with observed trends in the load-slip curves.
- The DTPT represents a cost-effective, easy-to-perform process that combines the simplicity of the large block pullout test procedure with the realistic distribution of bond mechanisms inherent in the flexural beam test.

7.13. RECOMMENDATIONS

The Direct Tension Pullout Test (DTPT) may be used at prestress/precast plants to evaluate the overall bond stress capacity for a particular combination of concrete, strand type, and prestressing conditions. Specimens may be fabricated in a prestressing bed directly in-line with the full sized beams that they represent. The test may be conducted using equipment already common to

prestress/precast plants—load cells and hydraulic jacks. Dead end slip may be determined using marking tape, a mark on the strand, or a dial gauge.

Testing criteria and "pass/fail" characteristics are based on aforementioned comparisons between the DTPT test and the benchmark flexural beam tests. A summary of those conclusions relative to the test recommendations is summarized below:

- The DTPT bond mechanism distribution was found to be similar, though not identical, to that of the flexural beam specimen.
- DTPT and flexural beam test load-slip curves had similar shapes, indicative of the presence of prestressing-related bond mechanisms.
- The strand-concrete bond along the embedment length of the DTPT test was found to be consistently weaker than that of the flexural beam as seen in Figure 13.
- A comparison of DTPT and flexural beam test bond stress-slip curves verified this conclusion, and the DTPT test load-slip curve was found to be consistently more conservative than that of the flexural beam test.
- Overlap of transfer and flexural bond lengths in the DTPT test provides leads to greater measured slips at a given load than would actually occur in a full-scale beam.

Based on the above conclusions, the DTPT will overstate the slip response to applied loads, and it will consequently provide a conservative evaluation of bond strength resistance. Because of the overstated response, potential bond problems associated with prestressing will not be masked.

A variation of Equation 3 may be used to evaluate the success or failure of the test:

$$f_{ps} \cdot A_s = \mu \cdot l_d \cdot SA \qquad \text{Equation 6}$$

Where f_{ps} = the predicted stress in the strand at the nominal bending moment capacity of the full sized beam [ksi], A_s = the cross sectional area of the strand [in^2], μ = the average uniform bond stress that must be achieved to prohibit bond failure at f_{ps} [ksi], l_d = the ACI predicted development length of the full scale beam [in], and SA = the surface area of the strand per inch of strand [in/in].

In essence, the specimen is designed for a strand embedment of l_d and subjected to a pullout force equal to $f_{ps}A_s$. If the bond at the strand-concrete interface maintains the load throughout a target amount of slip, the development length for which the beam is designed and the bond strength of the strand-concrete interface in the full-scale beam can be said to be sufficient.

Experimental results and other literature indicate that the ACI specifications for development length are conservative. Predicted development lengths that are too long will lead to long embedment lengths and "pass" values for the test that do not accurately indicate the bond stress response in the development length. The test, therefore, is best suited to evaluate scenarios where the full-scale beam is designed for development lengths shorter than those called for in the ACI code.

The test is best used to *predict* development lengths for combinations of different concrete mixes and strands, as described in the results and discussion chapter of this report. For these tests, specimens should be prepared that are identical (or shorter) than those prepared in the report. Rather than constructing a complete load-slip curve, the load-slip response at a dead end slip of 0.1" may be considered. The development length back-calculated from the average uniform bond stress at a dead-end slip of 0.1" is comparable on a 1:1 basis to the development length of a flexural beam specimen (or full-scale beam), as determined from the trends exhibited in Figure 13. Based on experimental results, it is expected that maximum average uniform bond stress will not be achieved in a DTPT specimen at a slip below 0.1". Using, Equation 6, a reasonably conservative value of development length can be determined for a full-size beam composed of the same unique concrete mix and prestressing strand combination.

7.14. REFERENCES

ACI Committee 209, "Prediction of Creep, Shrinkage, and Temperature Effects in Concrete Structures (ACI 209R-92)," American Concrete Institute, Farmington Hills, Mich., 1997, 47 pp.

ACI Committee 318, "Building Code Requirements for Reinforced Concrete (ACI 318-89) and Commentary (318R-89)," American Concrete Institute, Farmington Hills, Mich., 2005, 353 pp.

American Association of State Highway and Transportation Officials. "AASHTO LRFD Bridge Design Specifications," Washington, DC: May 2000.

ASTM International. A615, C39, C260, C494, C403, West Conshohocken, PA.

Commonwealth of Pennsylvania Department of Transportation, "Publication 408/2003 - Specifications," www.dot.state.pa.us, October 2004.

Daczko, J., A., "Stability of Self-Consolidating Concrete, Assumed or Ensured?," Conference Proceedings: First North American Conference on the Design and Use of Self-Consolidating Concrete, Master Builders, November 12-13, 2002.

Freyne, S.F., Russell, B.W., and Bush, T.D. Jr., "Heat Curing of High-Performance Concrete Containing Type III Cement," ACI Materials Journal, V.100, No.6, Nov.-Dec. 2003, p.449-454.

Geiseler, J., Kollo, H., and Lang, E., "Influence of Blast Furnace Cements on Durability of Concrete structures," ACI Materials Journal, V.92, No.3, May-June 1995, p.252-257.

Kosmatka, S.H. and Panarese, W.C., "Design and Control of Concrete Admixtures," Skokie, IL: Portland Cement Association, 1988.

Logan, D., R., 1997, "Acceptance Criteria for Bond Quality of Strand for Pretensioned Prestressed Concrete Applications," *PCI Journal*, V. 42 No.2, Mar-Apr., pp. 52-90.

Naito, C., Parent, G., Brunn, G., and Tate, T., "Comparative Performance of High Early Strength and Self Consolidating Concrete for Use in Precast Bridge Beam Construction," PITA Project PIT-457-04, ATLSS Report 05-03, Bethlehem, PA, June 2005.

PCI FAST Team, "Interim Guidelines for the Use of Self-Consolidating Concrete in Precast/Prestressed Concrete in Precast/Prestressed Concrete Institute Member Plants," TR-6-03, PCI, April 2003, pp.88.

Popovics, S., 1971, "Physical Aspects of the Setting Time of Portland Cement Concrete," Journal of Materials, JMLSA, Vol.6, No.1, March, pp.150-162.

Precast / Prestressed Concrete Institute. "Precast Prestressed Concrete Bridge Design Manual," Chicago: 1997.

8. APPENDIX A - NOTATION

A_s = Cross sectional area of prestressing strand [in^2]

SA = The surface area of the strand in terms of unit length [in^2/in]

CGC = Center of gravity of concrete [in]

CGS = Center of gravity of steel [in]

d_b = Diameter of prestressing strand [in]

d_p = Depth from top compression fiber of beam to center of gravity of strand [in]

E_c = Elastic modulus of concrete [ksi]

f'_c = Compressive strength of concrete [psi]

f_{pe} = Effective prestress in beam [ksi]

f_{ps} = Stress in strand upon failure of beam [ksi]

f_{pu} = Ultimate strength of prestressing strand [ksi]

f'_t = Splitting tensile strength of concrete [psi]

f'_r = Modulus of rupture of concrete [psi]

t = Time [days of hours]

l = Length of the strand-concrete bond

L_d = Development length of strand in bulb tee beam [in.]

l_d = Development length of strand in part 2

l_t = Transfer length [in]

M_{max} = Maximum applied moment in bulb tee beam [kip-in]

M_n = Nominal flexural resistance of beam using as-built material strengths [kip-in]

P = Applied load [kip]

PR = Penetration resistance of concrete

V_{max} = Maximum applied shear [kip]

V_n = Nominal shear resistance of beam using as-built material strengths [kip]

ε_{sh} = Shrinkage strain

μ = Bond stress [ksi]

μ_{msx} = The maximum bond strength at the strand-concrete interface [ksi]

v_{cr} = Creep coefficient

9. APPENDIX B-VITA

Name of Candidate:	Gregory Charles Parent
Place of Birth:	St. Paul, Minnesota, USA
Names of Parents:	Dale and JoAnn Parent
Institutions Attended:	Received Bachelors of Science in Civil Engineering from Lehigh University in spring 2003
Honors:	Member of the Chi Epsilon Civil Engineering Honor Society Member of the Fritz Engineering Research Society
Teaching Experience:	TA for CEE 10 under the direction of Professor Lennon TA for CEE 159 under the direction of Professor Naito TA for CEE 207 under the direction of Professor Lennon TA for CEE 262 under the direction of Professor Muller TA for CEE 262 under the direction of Professor Lu
Work Experience:	Project Manager for Structural Preservation Systems Hawthorne, NJ. June 2003-January 2004
Additional Information:	Greg sang with the Lehigh University choir for 11 semesters. Greg toured with the choir to the following countries: Russia, Germany, Austria, Hungary, Czech Republic, Holland and Finland. Greg is an avid competitor in the sport of Ultimate Frisbee. Was a member of the Lehigh Ultimate Frisbee Team for 5 years. Greg graduated from Lehigh and went to work for Martin/Martin, a Structural Design Firm in Denver Colorado.

END OF
TITLE